JACS
JOURNAL OF THE AMERICAN CHEMICAL SOCIETY
Communication
pubs.acs.org/JACS

Hierarchical Self-Assembly of a Copolymer-Stabilized Coacervate Protocell

Alexander F. Mason,[†] Bastiaan C. Buddingh',[†] David S. Williams,*[,†,§] and Jan C. M. van Hest*[,†]

[†]Eindhoven University of Technology, P.O. Box 513 (STO 3.31), 5600MB Eindhoven, The Netherlands
[§]Department of Chemistry, Swansea University, Swansea SA2 8PP, United Kingdom

Supporting Information

ABSTRACT: Complex coacervate microdroplets are finding increased utility in synthetic cell applications due to their cytomimetic properties. However, their intrinsic membrane-free nature results in instability that limits their application in protocell research. Herein, we present the development of a new protocell model through the spontaneous interfacial self-assembly of copolymer molecules on biopolymer coacervate microdroplets. This hierarchical protocell model not only incorporates the favorable properties of coacervates (such as spontaneous assembly and macromolecular condensation) but also assimilates the essential features of a semipermeable copolymeric membrane (such as discretization and stabilization). This was accomplished by engineering an asymmetric, biodegradable triblock copolymer molecule comprising hydrophilic, hydrophobic, and polyanionic components capable of direct coacervate membranization via electrostatic surface anchoring and chain self-association. The resulting hierarchical protocell demonstrated striking integrity as a result of membrane formation, successfully stabilizing enzymatic cargo against coalescence and fusion in discrete protocellular populations. The semipermeable nature of the copolymeric membrane enabled the incorporation of a simple enzymatic cascade, demonstrating chemical communication between discrete populations of neighboring protocells. In this way, we pave the way for the development of new synthetic cell constructs.

The design and engineering of mesostructured compartments that mimic aspects of cellular structural complexity is an important line of research that has received much recent attention.[1] So-called "protocells" present an opportunity to explore, in the laboratory, biochemical concepts such as compartmentalization, communication, metabolism, and replication, while shedding light upon prebiotic forms of early life.[2] Examples of such protocellular systems include cell-membrane mimetic structures such as vesicles comprising lipids, fatty acids, synthetic polymers, protein conjugates, or colloidal particles, alongside membrane-free examples of compartmentalization such as coacervates, aqueous two-phase systems (ATPS), and hydrogels.[3] Such systems have been employed in demonstrations of intra- and intercompartmental communication, compartmentalized transcription/translation, and growth/division.[1e,2b−f,3c,4] Principally, such protocells are realized through bottom-up engineering of diverse molecular components.[5] In some instances it is necessary to employ intricate protocols in order to direct protocell assembly toward the desired morphology. However, designing and realizing protocell models that arise through spontaneous self-assembly of molecular components reflects the physicochemical logic of life's emergence.[6]

Complex coacervate microdroplets, as a membrane-free protocell model, display a striking resemblance to intracellular phase separation processes.[7] Indeed, formation of cellular subcompartments via intermolecular self-organization is vital for cellular life.[8] However, the absence of a semipermeable membrane prevents such a system from evolving toward an out-of-equilibrium state.[9] Therefore, a critical aspect in the development of protocells is the interface between membrane-bound and membrane-free models: How can we create a single system that mimics both intracellular crowding and displays interfacial stabilization, employing a spontaneous assembly procedure? Seeking to explore the potential to engineer protocells with hierarchical complexity, the groups of both Mann and Keating have published elegant work demonstrating molecular organization, and membranization, at the external surface of membrane-free protocells.[3b−e,10] From such work the importance of careful balancing of molecular interactions in the engineering of such hybrid protocells is clear. With this in mind, the utilization of fatty acids and lipids in the hierarchical formation of a surface "membrane" is somewhat limited by chemical versatility, in contrast to their synthetic counterparts, amphiphilic block copolymers (BCPs). BCP vesicles (polymersomes) are a synthetic liposome mimic and, as such, are an interesting class of protocell in their own right.[3h,11] To this end, we have recently presented a multicompartmentalized protocell formed by encapsulation of BCP vesicles (polymersomes) within a giant polymersome in order to demonstrate intracellular communication between synthetic organelles.[3d]

Herein, we present the design and utilization of a biodegradable triblock copolymer (terpolymer) for the interfacial stabilization of cell-sized coacervate microdroplets, thereby creating a new hybrid protocell. First, we prepared a biodegradable coacervate comprising charged amylose derivatives, capable of undergoing complex coacervation under physiological conditions. A polymer-based system was chosen, as small molecule-based coacervates are sensitive toward buffer strength and dissociate under physiological conditions.[12] The

Received: October 11, 2017
Published: November 14, 2017

DOI: 10.1021/jacs.7b10846
J. Am. Chem. Soc. 2017, 139, 17309−17312

design concept underlying the self-assembly of terpolymer molecules on the biopolymer-dense coacervate surface relies upon a balance between (i) electrostatically driven coacervate anchoring, (ii) hydrophilic surface buoyancy, and (iii) hydrophobic membrane self-association (Figure 1). Terpolymer molecules comprising poly(ethylene glycol), poly(caprolactone-*gradient*-trimethylene carbonate) and poly(glutamic acid) (PEG-PCL*g*TMC-PGlu) were synthesized and their *in situ* organization, stabilizing coacervate microdroplets against coalescence and structural deformation, was confirmed. Having established the protocell platform we then demonstrate effective macromolecular discretization and show

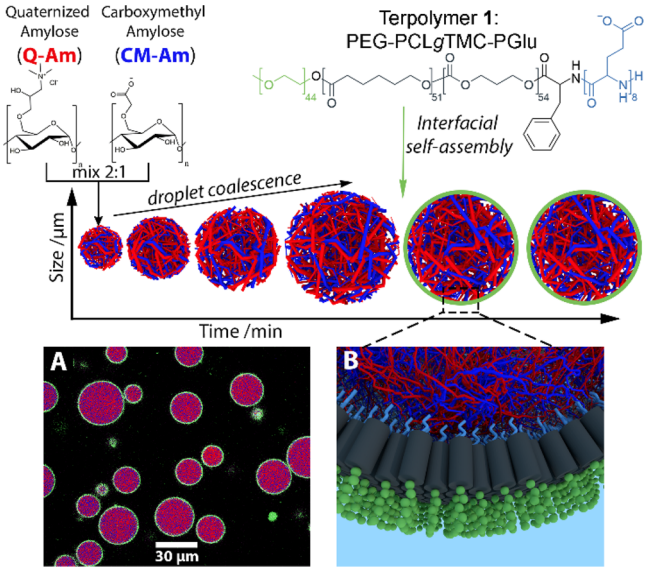

Figure 1. Hierarchical self-assembly of a terpolymer-stabilized coacervate protocell. Oppositely charged amylose biopolymers undergo complex coacervation and droplet formation, followed by interfacial self-assembly of terpolymer **1**. (A) Confocal micrograph of terpolymer/coacervate protocells with internalized BSA-FITC (purple) and terpolymer membrane (green, Nile Red). (B) 3D representation of interfacial assembly of terpolymers.

that mixed populations of protocells can coexist without exchanging contents, facilitating chemical communication.

Terpolymer synthesis was accomplished using a modular approach as presented in the literature for similar macromolecules.[13] A diblock copolymer of PEG (2 kDa) and PCL*g*TMC (ca. 10.8 kDa) was prepared,[14] to which a short PGlu (ca. 8 or 9 repeats) was added using *N*-carboxy anhydride polymerization (Figures S1 and S2).[15] Following the aforementioned design scheme: (i) Polyanionic PGlu can engage in long-range electrostatic interactions with the coacervate surface, providing an anchoring effect. (ii) Hydrophobic PCL*g*TMC retains the flexibility (due to its non-glassy nature) necessary to undergo dynamic reorganization upon coacervate surface interaction, while driving hydrophobic chain association. (iii) 2 kDa coronal PEG chains are necessary to prevent sequestration of terpolymer molecules into the coacervate phase, providing steric buoyancy. Preparation of the oppositely charged coacervate components was accomplished using linear $\alpha(1\rightarrow4)$-amylose.[16] Charged derivatives of polysaccharides, such as amylose, are widely used in biomaterials engineering.[17] The degree of modification was tailored to emphasize the cationic properties of the coacervate

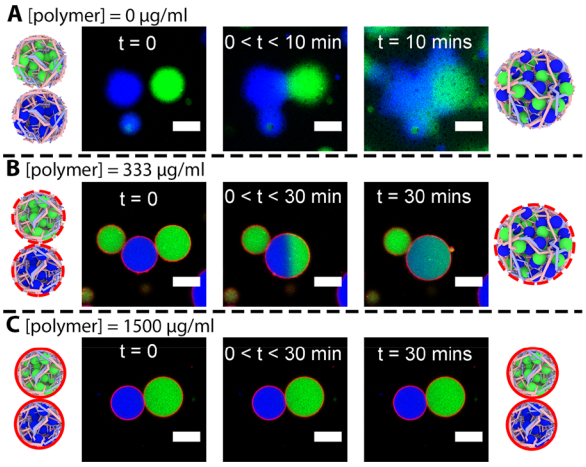

Figure 2. Membrane stabilization and mixing study. Populations of coacervate droplets containing either BSA-FITC (green) or BSA-Cy5 (blue) were mixed after treatment with different amounts of terpolymer **1**; the presence of a membrane was visualized with Nile Red (red). (A) Without terpolymer addition unstable coacervates mix immediately. Terpolymer addition of (B) 333 and (C) 1500 μg/mL resulted in slowed mixing or nonmixing, respectively (scale bars = 10 μm).

phase, with quaternized amylose (Q-Am) prepared with a degree of substitution (DS) of 2 and carboxymethylated amylose (*Cm*-Am) with a DS of 1 (Figure S3). Coacervation was initiated by mixing aqueous solutions of Q-Am and *Cm*-Am in phosphate-buffered saline (PBS) and detected by solution turbidity. Maximal coacervation was observed at mixtures of Q-Am:*Cm*-Am ranging from 2:1 to 1:2 (Figure S4a). Using a 2:1 coacervate stoichiometry, to accentuate the positive charge of the coacervate droplets, we observed coacervation up to a [NaCl] $\approx$ 200 mM above PBS and a zeta-potential of ca. +30 mV (Figure S4b,c). Without interfacial stabilization, coacervate droplets were unstable and coalesced rapidly (Figure 2A).

To assess the ability of terpolymer **1** to undergo interfacial self-assembly, we added small volumes of a DMSO solution directly to a coacervate suspension after 2 min of mixing. It was immediately apparent that interfacial assembly and membranization occurred due to the strong fluorescent signal of Nile Red at the external interface of the coacervate droplets. Addition of increasing concentrations of terpolymer **1** had a marked effect on coacervate stability; transforming unstable, readily deforming "blobs" into discrete spheroids that did not wet on the glass surface (Figure 2). Rough calculations, approximating coacervate density as 1.1 g/mL and its volume as ca. 1 vol% at these concentrations, gave an estimate of 1×10^7 droplets per mL (having an average diameter of 20 μm).[12b] This gave a total coacervate surface area in the region of 10^{15}–10^{16} nm^2 per mL. With each terpolymer chain occupying ca. 1 nm^2, the addition of 333 μg/mL of terpolymer (yielding ca. 10^{14} molecules per mL) was expected to give incomplete coverage, which was supported by our observations (Figure S6a). Moreover, increasing the amount of terpolymer added by almost 5-fold (yielding ca. 10^{15} molecules per mL) appeared to provide sufficient coacervate coverage to provide complete membranization, in-line with our calculations (Figure S6b). Control over protocell fabrication was exemplified by our ability to arrest coacervate coalescence and growth by adding terpolymer at different time points. Protocells with sizes of 5.23 $\pm$ 0.95, 22.7 $\pm$ 5.9, and 39.3 $\pm$ 9.6 μm were generated by addition of

DOI: 10.1021/jacs.7b10846
J. Am. Chem. Soc. 2017, 139, 17309–17312

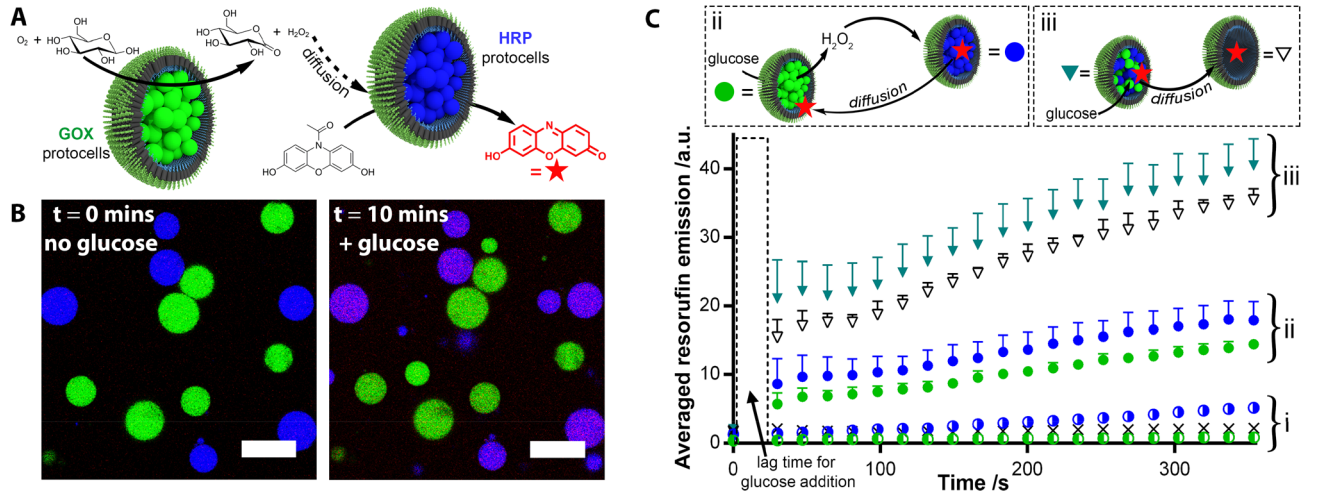

Figure 3. Demonstration of chemical communication between protocell populations. (A) Representation of the GOX/HRP enzyme cascade encapsulated in two protocell subpopulations, identified by FITC (green) or Cy5 (blue), respectively, with H_2O_2 being the content of this molecular conversation. (B) Example of confocal data obtained; resorufin (red) is produced preferentially in HRP-protocells changing them from blue to purple (scale bars = 20 μm). (C) Analysis of the average resorufin fluorescence in subpopulations of protocells: (i) Background levels of resorufin production were measured using GOX-protocells only, HRP-protocells only, or a mixture without glucose addition as controls (green half-spheres, blue half-spheres, or crosses, respectively). (ii) Increasing resorufin fluorescence in either GOX- or HRP-protocells in a mixed system (green or blue spheres, respectively). (iii) Increasing resorufin fluorescence in co-encapsulated GOX/HRP-protocells mixed with empty protocells (filled or empty triangles, respectively).

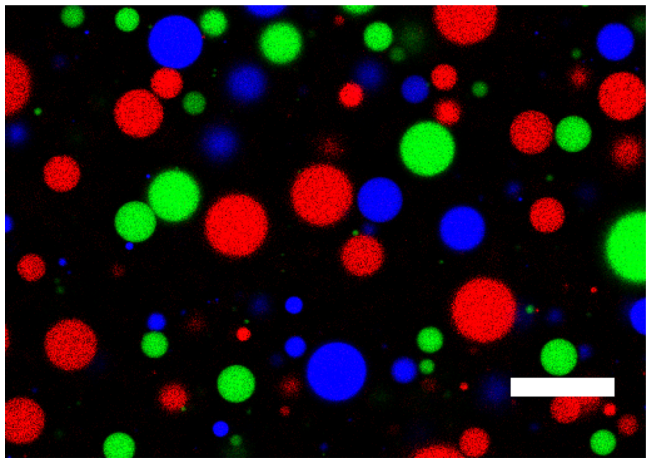

Figure 4. Three separate protocell populations encapsulating fluorescently labeled BSA with either FITC (green), Cy5 (blue), or RITC (red), persistent for 2.5 h after mixing (scale bar = 20 μm).

terpolymer after 15 s, 2 min, or 5 min, respectively (Figure S5). In this way, we have achieved membrane-stabilized complex coacervates via the interfacial organization of a terpolymer using a process based solely on self-assembly.

To probe protocell integrity and coalescence behavior, mixing experiments were performed. Fluorescently labeled BSA (FITC or Cy5), succinylated to drive complete coacervate uptake (confirmed spectroscopically), was sequestered into separate protocell populations. After terpolymer addition to the separate populations, they were mixed in a confocal dish and coalescence monitored with time (Figure 2). As expected, uncoated coacervates readily mix and deform in an uncontrolled fashion (Figure 2A). With suboptimal [terpolymer **1**] added (333 μg/mL), partial stability was imparted to the system, with droplets maintaining shape and contents mixing at slower time scales (Figure 2B). With optimal [terpolymer **1**] (1500 μg/mL) microdroplets were stable over longer periods of time and displayed no content mixing, even after 2.5 h (Figure 2C and Figure 4 below).

In order to demonstrate the life-like potential of this system, an enzymatic cascade was employed to demonstrate chemical communication (Figure 3A). Glucose oxidase (GOX) and horseradish peroxidase (HRP) were incorporated into two subpopulations of protocells or co-encapsulated in a single population. In this way we demonstrate protocell communication, where hydrogen peroxide (H_2O_2) is transferred between compartments in order to activate Amplex Red peroxidation, and contrast that to a dual-functionalized protocell population. Again, enzymes were fluorescently labeled (FITC-GOX and Cy5-HRP) and succinylated to enhance coacervate uptake. In contrast to other copolymeric membranes, PCL*g*TMC was semipermeable toward small molecules, eliminating the need for insertion of porins or similar proteins.[18] This means that the substrate (β-D-glucose) can freely transpose the membrane, whereas macromolecular cargo cannot (Figure 2C). Reaction progress was monitored by the fluorescence of the product, resorufin, distinguishing it from enzyme signals by appropriately gating the excitation/emission wavelengths of the confocal microscope (Figure 3C). From the dual-population experiment, resorufin fluorescence was observed to initially increase in the HRP-protocell population and, thereafter, appeared in the GOX-protocells, at a slower rate. Control experiments showed no background activity, so the origin of resorufin fluorescence in the GOX-protocell population was due to molecular diffusion. Although it is evidently originating in the HRP-protocells, resorufin can cross the semipermeable membrane and re-equilibrates throughout the entire protocell population (being effectively sequestered by the coacervate phase as evidenced by the low background fluorescence). Resorufin production in the co-encapsulated protocell population occurred at a rate around 2-fold higher than in the protocells in which the enzymes were separated (Figure 3C). In order to evaluate resorufin diffusion from this system we added nonfunctional FITC-BSA protocells into the solution. In

DOI: 10.1021/jacs.7b10846
J. Am. Chem. Soc. 2017, 139, 17309−17312

much the same way as for the GOX-protocells in the former experiment, resorufin fluorescence inside these nonactive protocells lagged behind the active protocells.

This Communication highlights the potential of the terpolymer-stabilized coacervate protocells for the investigation of biomolecular processes in crowded, discrete environments. For example, numerous components can be encapsulated and spatially ordered in order to study complex multicomponent processes on extended time scales, as exemplified in Figure 4 (see also Figure S6). There is tremendous scope for further development of this system to support increasingly complex synthetic cell applications.

■ ASSOCIATED CONTENT

Supporting Information

The Supporting Information is available free of charge on the ACS Publications website at DOI: 10.1021/jacs.7b10846.

Experimental details and characterization data, including Figures S1−S6 (PDF)

■ AUTHOR INFORMATION

Corresponding Authors

*d.s.williams@swansea.ac.uk

*j.c.m.v.hest@tue.nl

ORCID

Bastiaan C. Buddingh': 0000-0003-4411-9145

David S. Williams: 0000-0002-8209-6899

Jan C. M. van Hest: 0000-0001-7973-2404

Notes

The authors declare no competing financial interest.

■ ACKNOWLEDGMENTS

Authors acknowledge the support from the Ministry of Education, Culture and Science (Gravitation program 024.001.035) and the ERC Advanced grant Artisym 694120.

■ REFERENCES

(1) (a) Li, M.; Huang, X.; Tang, T. Y. D.; Mann, S. *Curr. Opin. Chem. Biol.* **2014**, *22*, 1−11. (b) Brea, R. J.; Hardy, M. D.; Devaraj, N. K. *Chem. - Eur. J.* **2015**, *21*, 12564−12570. (c) Balasubramanian, V.; Herranz-Blanco, B.; Almeida, P. V.; Hirvonen, J.; Santos, H. A. *Prog. Polym. Sci.* **2016**, *60*, 51−85. (d) Trantidou, T.; Friddin, M.; Elani, Y.; Brooks, N. J.; Law, R. V.; Seddon, J. M.; Ces, O. *ACS Nano* **2017**, *11*, 6549−6565. (e) Buddingh', B. C.; van Hest, J. C. M. *Acc. Chem. Res.* **2017**, *50*, 769−777.

(2) (a) Crosby, J.; Treadwell, T.; Hammerton, M.; et al. *Chem. Commun.* **2012**, *48*, 11832−11834. (b) Sokolova, E.; Spruijt, E.; Hansen, M. M. K.; Dubuc, E.; Groen, J.; Chokkalingam, V.; Piruska, A.; Heus, H. a; Huck, W. T. S. *Proc. Natl. Acad. Sci. U. S. A.* **2013**, *110*, 11692−11697. (c) Elani, Y.; Law, R. V.; Ces, O. *Nat. Commun.* **2014**, *5*, 5305. (d) Ichihashi, N.; Yomo, T. *Curr. Opin. Chem. Biol.* **2014**, *22*, 12−17. (e) Tang, T.-Y. D.; van Swaay, D.; deMello, A.; Ross Anderson, J. L.; Mann, S. *Chem. Commun.* **2015**, *51*, 11429−11432. (f) Lentini, R.; Yeh Martín, N.; Mansy, S. S. *Curr. Opin. Chem. Biol.* **2016**, *34*, 53−61.

(3) (a) de Hoog, H.-P. M.; Nallani, M.; Tomczak, N. *Soft Matter* **2012**, *8*, 4552. (b) Williams, D. S.; Patil, A. J.; Mann, S. *Small* **2014**, *10*, 1830−1840. (c) Dewey, D. C.; Strulson, C. A.; Cacace, D. N.; Bevilacqua, P. C.; Keating, C. D. *Nat. Commun.* **2014**, *5*, 4670. (d) Peters, R. J. R. W.; Marguet, M.; Marais, S.; Fraaije, M. W.; van Hest, J. C. M.; Lecommandoux, S. *Angew. Chem., Int. Ed.* **2014**, *53*, 146−150. (e) Dora Tang, T.-Y.; Rohaida Che Hak, C.; Thompson, A. J.; Kuimova, M. K.; Williams, D. S.; Perriman, A. W.; Mann, S. *Nat. Chem.* **2014**, *6*, 527−533. (f) Baxani, D. K.; Morgan, A. J. L.; Jamieson, W. D.; Allender, C. J.; Barrow, D. A.; Castell, O. K. *Angew. Chem., Int. Ed.* **2016**, *55*, 14240−14245. (g) Deng, N.-N.; Yelleswarapu, M.; Huck, W. T. S. *J. Am. Chem. Soc.* **2016**, *138*, 7584−7591. (h) Mason, A. F.; Thordarson, P. *J. Polym. Sci., Part A: Polym. Chem.* **2017**, *55*, 3817−3825. (i) Mytnyk, S.; Olive, A. G. L.; Versluis, F.; Poolman, J. M.; Mendes, E.; Eelkema, R.; van Esch, J. H. *Angew. Chem., Int. Ed.* **2017**, *56*, 1−7.

(4) (a) Xu, J.; Sigworth, F. J.; LaVan, D. A. *Adv. Mater.* **2010**, *22*, 120−127. (b) Grzybowski, B. A.; Huck, W. T. S. *Nat. Nanotechnol.* **2016**, *11*, 585−592. (c) Rodríguez-Arco, L.; Li, M.; Mann, S. *Nat. Mater.* **2017**, *16*, 857−863.

(5) (a) Dzieciol, A. J.; Mann, S. *Chem. Soc. Rev.* **2012**, *41*, 79. (b) Grover, M.; He, C.; Hsieh, M.-C.; Yu, S.-S. *Processes* **2015**, *3*, 309−338.

(6) Mann, S. *Angew. Chem., Int. Ed.* **2008**, *47*, 5306−5320.

(7) (a) Brangwynne, C. P.; Tompa, P.; Pappu, R. V. *Nat. Phys.* **2015**, *11*, 899−904. (b) Banani, S. F.; Lee, H. O.; Hyman, A. A.; Rosen, M. K. *Nat. Rev. Mol. Cell Biol.* **2017**, *18*, 285−298.

(8) (a) Brangwynne, C. P. *Soft Matter* **2011**, *7*, 3052. (b) Brangwynne, C. P. *J. Cell Biol.* **2013**, *203*, 875−881. (c) Shin, Y.; Brangwynne, C. P. *Science* **2017**, *357*, 1253.

(9) Jia, T. Z.; Hentrich, C.; Szostak, J. W. *Origins Life Evol. Biospheres* **2014**, *44*, 1−12.

(10) (a) Helwa, Y.; Dave, N.; Liu, J. *Soft Matter* **2013**, *9*, 6151−6158. (b) Aumiller, W. M.; Pir Cakmak, F.; Davis, B. W.; Keating, C. D. *Langmuir* **2016**, *32*, 10042−10053.

(11) Peters, R. J. R. W.; Louzao, I.; van Hest, J. C. M. *Chem. Sci.* **2012**, *3*, 335−342.

(12) (a) Koga, S.; Williams, D. S.; Perriman, A. W.; Mann, S. *Nat. Chem.* **2011**, *3*, 720−724. (b) Williams, D. S.; Koga, S.; Hak, C. R. C.; Majrekar, A.; Patil, A. J.; Perriman, A. W.; Mann, S. *Soft Matter* **2012**, *8*, 6004.

(13) (a) Deng, C.; Rong, G.; Tian, H.; Tang, Z.; Chen, X.; Jing, X. *Polymer* **2005**, *46*, 653−659. (b) Deng, C.; Tian, H.; Zhang, P.; Sun, J.; Chen, X.; Jing, X. *Biomacromolecules* **2006**, *7*, 590−596.

(14) (a) Couffin, A.; Delcroix, D.; Martín-Vaca, B.; Bourissou, D.; Navarro, C. *Macromolecules* **2013**, *46*, 4354−4360. (b) Campos, J. M.; Ribeiro, M. R.; Ribeiro, M. F.; Deffieux, A.; Peruch, F. *Eur. Polym. J.* **2013**, *49*, 4025−4034.

(15) Zou, J.; Fan, J.; He, X.; Zhang, S.; Wang, H.; Wooley, K. L. *Macromolecules* **2013**, *46*, 4223−4226.

(16) (a) Heinze, T.; Rensing, S.; Koschella, A. *Starch - Stärke* **2007**, *59*, 199−207. (b) Amar-Lewis, E.; Azagury, A.; Chintakunta, R.; Goldbart, R.; Traitel, T.; Prestwood, J.; Landesman-Milo, D.; Peer, D.; Kost, J. *J. Controlled Release* **2014**, *185*, 109−120.

(17) Mizrahy, S.; Peer, D. *Chem. Soc. Rev.* **2012**, *41*, 2623−2640.

(18) (a) Garni, M.; Thamboo, S.; Schoenenberger, C.-A.; Palivan, C. G. *Biochim. Biophys. Acta, Biomembr.* **2017**, *1859*, 619−638. (b) Larrañaga, A.; Lomora, M.; Sarasua, J. R.; Palivan, C. G.; Pandit, A. *Prog. Mater. Sci.* **2017**, *90*, 325−357.

DOI: 10.1021/jacs.7b10846
J. Am. Chem. Soc. 2017, 139, 17309−17312